

Microscopic description of insulator-metal transition in high-pressure oxygen

Luis Craco¹, Mukul S. Laad² & Stefano Leoni³

¹Instituto de Física, Universidade Federal de Mato Grosso, 78060-900, Cuiabá, MT, Brazil. ²The Institute of Mathematical Sciences, C.I.T. Campus, Chennai 600 113, India. ³School of Chemistry, Cardiff University, Cardiff, CF10 3AT, UK.

Unusual metallic states involving breakdown of the standard Fermi-liquid picture of long-lived quasiparticles in well-defined band states emerge at low temperatures near correlation-driven Mott transitions. Prominent examples are ill-understood metallic states in d - and f -band compounds near Mott-like transitions. Finding of superconductivity in solid O_2 on the border of an insulator-metal transition at high pressures close to 96 GPa is thus truly remarkable. Neither the insulator-metal transition nor superconductivity are understood satisfactorily. Here, we undertake a first step in this direction by focussing on the pressure-driven insulator-metal transition using a combination of first-principles density-functional and many-body calculations. We report a striking result: the finding of an orbital-selective Mott transition in a pure p -band elemental system. We apply our theory to understand extant structural and transport data across the transition, and make a specific two-fluid prediction that is open to future test. Based thereupon, we propose a novel scenario where soft multiband modes built from microscopically coexisting itinerant and localized electronic states are natural candidates for the pairing glue in pressurized O_2 .

I. INTRODUCTION

The unique properties of high-pressure induced solid phases of molecular gases continue to evince keen and enduring interest in condensed matter physics. Beginning with early ideas of Mott¹ and extending up to modern times², ideas of pressure-induced electronic, magnetic and structural transitions and possible superconductivity in such systems even provided early ground for strongly correlated systems, are currently a frontline research topic in condensed matter. Particularly interesting examples of intriguing physics in solidized molecular phases of gases are dense hydrogen³ and solid oxygen^{4,5}, as well as the most recent report of very high- T_c superconductivity in solid H_2S under very high pressure⁶. H_2 is predicted to metallize under high pressure, while solid O_2 even shows a superconducting phase ($T_c = 0.6$ K) at the border of a pressure-driven transition from a non-magnetic insulator to paramagnetic metal, joining the long list of materials exhibiting superconductivity proximate to metal-insulator transitions.

Pressurized molecular oxygen forms various low-temperature solid phases under pressure, labelled α , δ , ϵ and ζ phases⁷. At lower pressure, the antiferromagnetically ordered α phase transforms into another antiferromagnetically ordered δ phase at 5.4 GPa, followed by a non-magnetic ϵ phase at 8 GPa. Higher pressure, $P \simeq 96$ GPa, metallizes the system⁸, followed by emergence of superconductivity below $T_c \simeq 0.6$ K⁹. This astounding behavior in a molecular system, reminiscent of strongly correlated, doped Mott insulators in d -band oxides like cuprates, presents a significant challenge for theory. The high- P $\epsilon - \zeta$ phase transition is also accompanied by significant volume reduction¹⁰, with a contraction of about 10% of the lattice parameter along the b direction. The ϵ phase retains the layered nature of the lower pressure phases⁴, and the monoclinic ($C2/m$) structure^{10,11} as shown in Fig. 1.

That the driving force for the $\alpha - \beta$ transition at moderate T is dominantly magnetic has been established in a series of careful studies¹²⁻¹⁴. Indeed, early work of da Silva and Falicov¹⁵ already explained the measured heat of formation at the $\alpha - \beta$ transition in terms of the entropy difference computed from cluster analysis of a multi-orbital Hubbard model (or an equivalent $S = 1$ Heisenberg-like model in $d = 2$ dimensions). Observation of very different magnetic orders in the α, β phases, correlation between magnetic and structural changes along with ferromagnetic coupling between the off-plane near neighbors in the δ phase are reminiscent of those found in classic multi-band systems like V_2O_3 ¹⁶, taken together with the above, favor a multi-orbital description. Additional evidence for multi-orbital effects is provided by the anisotropic and partially discontinuous pressure-induced changes in the lattice parameters in the different phases^{11,17}. In such a scenario, increasing pressure is expected, in the simplest approximation, to decrease lattice spacings and increase the carrier itinerance. The result would then be to suppress antiferromagnetic order along with insulating behavior, and to induce metalization. In solid O_2 , antiferromagnetic order is destroyed well before metalization occurs¹⁸, and so, within the p^4 configuration of oxygen, the insulator-metal transition across the $\epsilon - \zeta$ transition must be regarded as a Mott metal-insulator transition. This suggests that on the one extreme, a Heisenberg model description is only valid in the insulating α, β, δ phases, and that a more general multi-orbital Hubbard model must be used, at least for the ϵ phase. At the other extreme, one-electron band structure calculations for the antiferromagnetically ordered phases do provide qualitatively correct ground states¹⁹. In addition, electronic structure calculation based on generalized gradient approximation (GGA) shows that the nonmagnetic insulating state is energetically favored at pressures corresponding to the ϵ -phase^{20,21}. However, by construction, *ab initio* density-functional calculations have intrinsic difficulties in describing non-magnetic insulating phases, and in particular the ϵ phase^{22,23}, for reasons described in detail in ref. 24. The observation of superconductivity at the border of this (Mott) insulator-to-metal transition thus

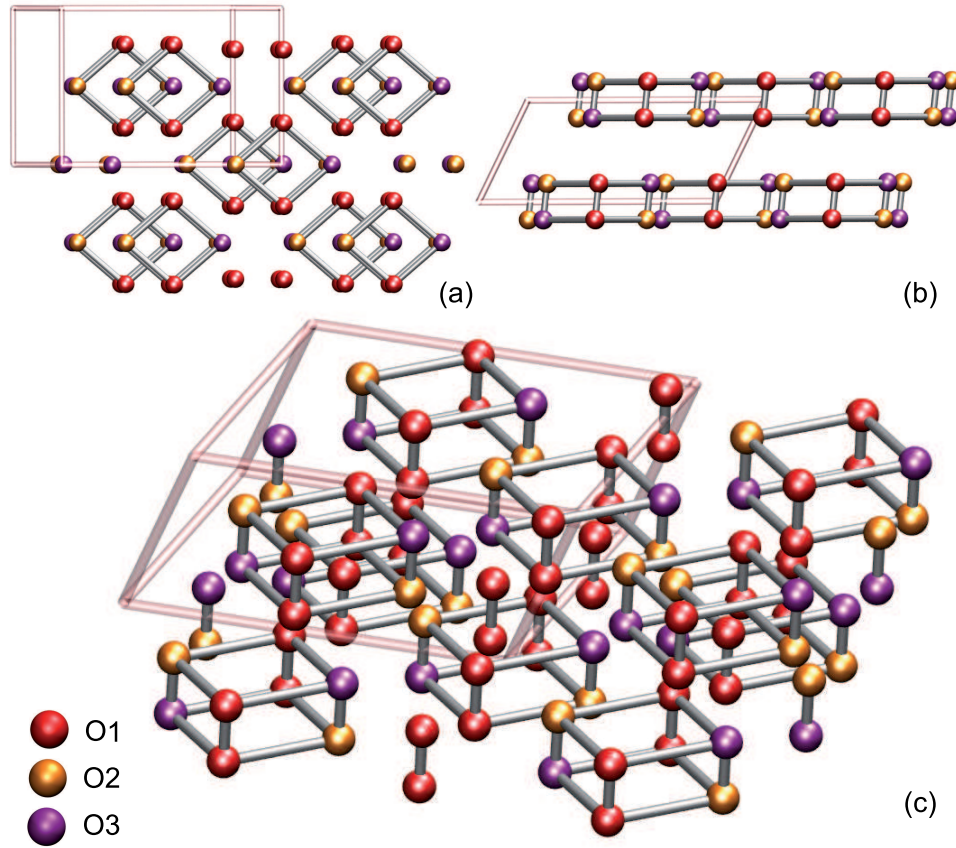


Figure 1 | Crystal structure of the ϵ -phase of solid oxygen. The structure as viewed perpendicular to the $a - b$ (a) and $a - c$ (b) planes. The O_8 clusters in the monoclinic unit cell (rose lines) are shown in (c). $O_x(x = 1, 2, 3)$ label the three inequivalent oxygen atoms.

suggests that dualistic behavior of correlated carriers (Mottness) near the insulator-metal transition is very likely implicated in the pairing glue. Thus, a search for the microscopic origin of the pair glue must involve understanding of the insulator-metal transition around 96 GPa.

Before presenting our local-density-approximation plus dynamical-mean-field (LDA+DMFT) results, we point out essential differences between band and Mott insulators. In conventional semiconductors (or band insulators) all bands below the Fermi energy are filled and, therefore, inert. Removing an electron leads to an empty state which can be thought of as a hole moving freely through the solid. The same is true for an added electron, which occupies the first empty band. In a multi-orbital Mott-Hubbard insulator, the insulating state arises because electron hopping from one site to another is inhibited by intra- and inter-orbital Coulomb repulsions. In these systems, when the band filling is slightly reduced from its commensurate value, a small number of unoccupied states are created; similarly adding electrons creates locally doubly occupied electronic states. The crucial difference in this case is that since the doped carriers can have either spin (\uparrow, \downarrow) with equal probability, doping a Mott insulator, *e.g.*, by holes, creates two available states at the Fermi energy. This is at the heart of spectral weight transfer, a phenomenon ubiquitous to Mott, as opposed to band, insulators. In both cases, electron hopping might still be prevented by inter-orbital Coulomb interactions in a multiband system. The resulting metallic state upon doping can vary from a Fermi liquid at weak coupling to an exotic orbital-selective, non-Fermi liquid metal for stronger electron-electron interactions, as doping and temperature²⁵ are varied. This fundamental difference between band and multi-orbital Mott-Hubbard insulators is of basic and practical interest. Below we show that sizable multiband electronic interactions are the clue to the insulating state of the ϵ -phase of solid oxygen and its evolution to a non-Fermi liquid metallic state at high pressures.

Possibility of Mott-Hubbard physics in purely p ²⁶⁻²⁹ or s ³⁰ band systems is very intriguing, since the naive expectation dictates that the itinerance (kinetic energy of p, s -carriers) is appreciable compared to the electron-electron interactions, as distinct from d -band systems, where the d electrons reside in much narrower bands (hence the effective U/W is sizable; U and W are, respectively, the on-site Coulomb repulsion and the bare one-particle band width)³¹. Thus, understanding Mottness in solidified gases with active p or s bands is undoubtedly an issue of great contemporary interest. In light of the discussion above, we study how an orbital-selective interplay between appreciable p -band itinerance and sizable, on-site Coulomb repulsion, U , plays a central role in this unique Mott transition in solid O_2 .

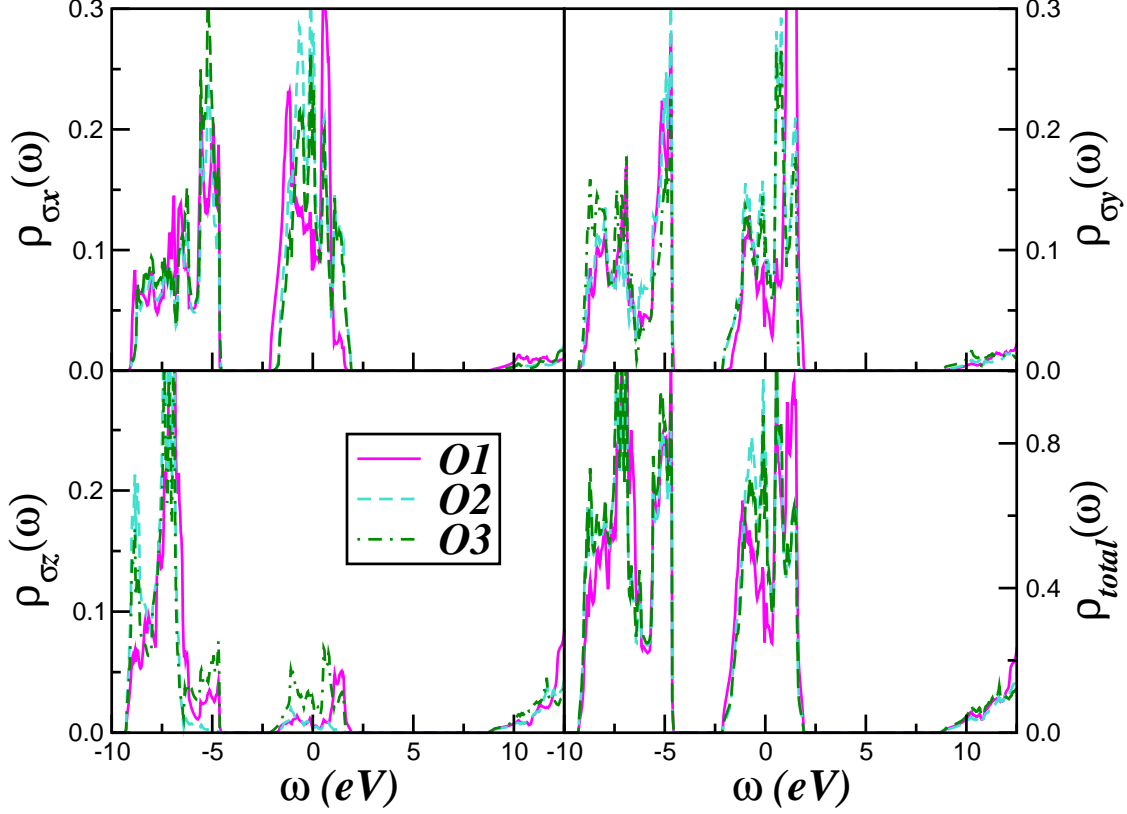


Figure 2 | Orbital resolved and total LDA density-of-states (DOS) for the three inequivalent oxygen atoms in the ϵ -phase. Notice that all bands as well span over the Fermi level. Also relevante is the evolution of the electronic DOS at different polarizations.

II. RESULTS

Electronic Structure

To quantify the correlated electronic structure of solid O_2 , we start with the $C2/m$ structure (Fig. 1) with lattice parameters derived in ref. 11. Here, local-density approximation (LDA) calculations for the real crystal structure of the ϵ -phase were performed using the linear muffin-tin orbitals (LMTO)^{32,33} scheme in the atomic sphere approximation³⁴. The corresponding LDA density-of-states of the three (symmetry) inequivalent atoms^{4,11} is shown in Fig. 2. Strong intramolecular overlap leads to propensity to localization of the p_z , i.e. the σ -orbital^{19,35} in the energy level diagram of O_2 . However, due to inter-molecular orbital overlap in the monoclinic structure, the p_z states acquire some itinerance, explaining the small amount of p_z states found at the Fermi energy. As seen in Fig. 2, all π -bands cross the Fermi energy, providing a metallic state within LDA.

Within LDA, the one-electron part of the many-body Hamiltonian for solid oxygen is now $H_0 = \sum_{\mathbf{k},a,\sigma} \epsilon_a(\mathbf{k}) c_{\mathbf{k},a,\sigma}^\dagger c_{\mathbf{k},a,\sigma} + \sum_{i,a,\sigma} \Delta_a n_{i\sigma}^a$, where $a = x, y, z$ label the three diagonalized p orbitals and the Δ_a are on-site orbital energies in the real structure of solid O_2 . In light of antiferromagnetic insulator¹⁵ phases and the non-magnetic Mott transition, local multi-orbital interactions are mandatory to understand O_2 . These constitute the interaction terms $H_{int} = U \sum_{i,a} n_{i\uparrow}^a n_{i\downarrow}^a + U' \sum_{i,a \neq b} n_i^a n_i^b - J_H \sum_{i,a \neq b} \mathbf{S}_{ia} \cdot \mathbf{S}_{ib}$. Here, U ($U' \equiv U - 2J_H$) is the intra- (inter-) orbital Coulomb repulsion and J_H is the Hund's rule term. Following da Silva and Falicov¹⁵, we use $U = 11.6$ eV and $J_H = 0.45$ eV, along with the LDA bands of the three inequivalent oxygen atoms described above. In this work, the correlated multi-orbital problem of solid O_2 encoded in $H = H_0 + H_{int}$ is treated within the state-of-the-art local-density-approximation plus dynamical-mean-field-theory (LDA+DMFT) scheme³⁶. The DMFT self-energy, $\Sigma_a(\omega)$, requires a solution of the multi-orbital quantum impurity problem self-consistently embedded in an effective medium³⁶. We use the multi-orbital iterated-perturbation-theory (MO-IPT) as an impurity solver for DMFT³⁷: This analytic solver has a proven record of successes in describing finite temperature Mott transitions³⁸ as well as unconventional behavior in correlated p -band systems³⁹⁻⁴¹.

With orbital orientation-induced anisotropic LDA one-particle energies and hoppings, multi-orbital correlations renormalize various p -bands in different ways. Generically, one expects partial (Mott) localization of a subset of bands, leading to orbitally selective Mott transitions, and bad metallic states^{31,38,42}. Within LDA+DMFT, this orbital-selective mechanism involves two renormaliza-

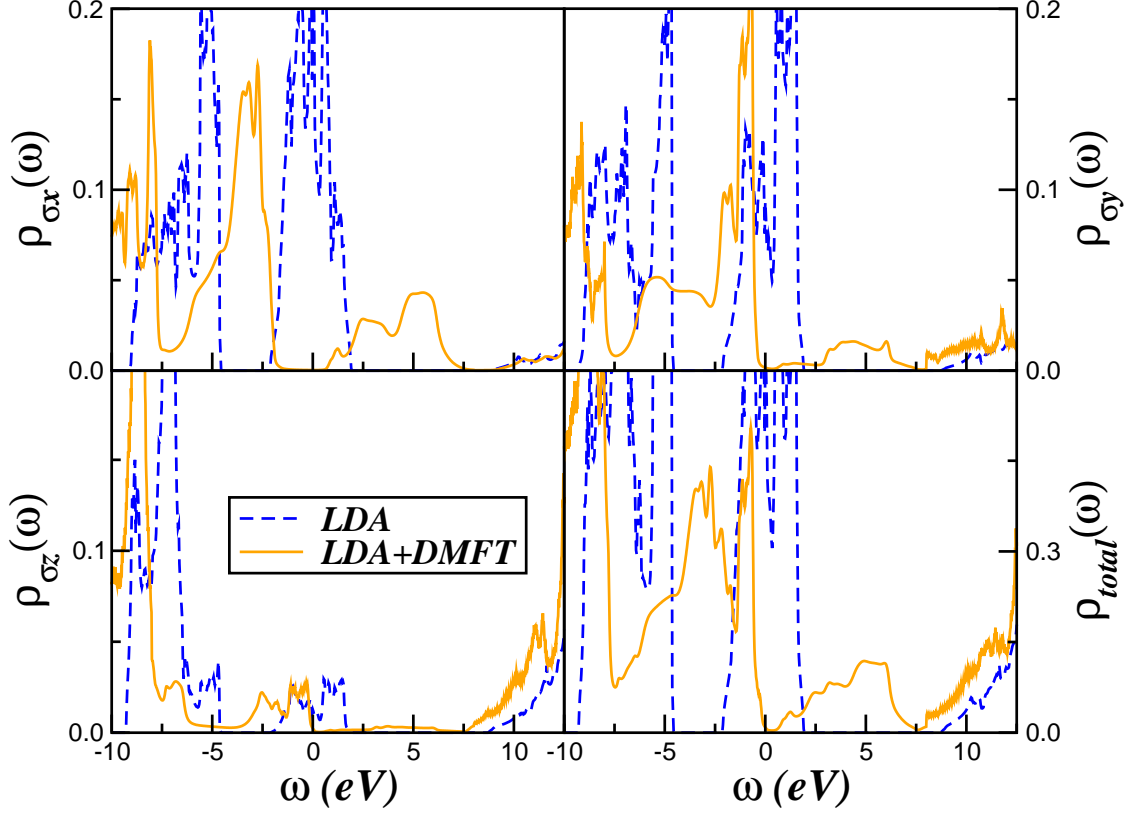


Figure 3 | Comparison between the LDA and LDA+DMFT orbital-resolved and total density-of-states in the ε -phase of solid O_2 . LDA+DMFT results for the Mott insulating ε phase of oxygen were obtained using the intra- (inter-) orbital Coulomb repulsion, $U = 11.6$ eV ($U' = 10.7$ eV) and the Hund's rule interaction $J_H = 0.45$ eV for the total band filling, $n=4$. Large-scale transfer of spectral weight from low energy to high energies is visible in the correlated spectral functions of the p_x and p_y bands. Also clear is the destruction of the low-energy peak of the p_z in LDA.

tions: static (multi-orbital Hartree) renormalization shifts the p -bands relative to each other by amounts depending upon their *bare* on-site orbital energies (Δ_a) and occupations (n^a). In addition, dynamical effects of $U, U' \equiv U - 2J_H$ drive large spectral weight transfer over wide energy scales^{38,42}. The large, anisotropic changes in dynamical spectral weight transfer in response to small changes in bare one-particle (LDA) parameters (for example, crystal-field splittings under pressure)³⁸ are known to drive the orbital-selective Mott transition in real multi-orbital systems. As we show below, precisely such an orbital-selective Mott transition, accompanied by an incoherent metallic phase in solid O_2 , occurs at very high pressures.

Using U, U', J_H as obtained in ref. 15, we find that the ε phase is a Mott insulator, as shown in Fig. 3. The size of the charge gap is orbital dependent, and is larger for the p_x band compared to the other two. Large spectral weight transfer, characteristic of dynamical local correlations, is explicitly manifested in the qualitative difference between LDA and LDA+DMFT spectra. At first sight, derivation of a Mott insulator with $U < W$ in solid O_2 seems a bit puzzling. The reason, however, is that, in this multi-orbital system, both U, U' are appreciable, and the combined effect of both acting in tandem is to (i) reduce the band-width of each band (this can arise solely from U , even for the artificial case of $U' = 0$), and (ii) the dominant effect of U' on a reduced bandwidth is to split the bands via the Mott mechanism. In the actual multi-orbital problem, both effects are simultaneously operative, and reinforce each other.

From our results in Fig. 3, we compute the renormalized orbital splittings (δ_a) and occupations (n^a) within LDA and LDA+DMFT. Within LDA, we find $(\delta_x, \delta_y, \delta_z) = (-1.12, -0.95, -5.22)$ eV and $(n_\sigma^x, n_\sigma^y, n_\sigma^z) = (0.68, 0.59, 0.53)$. LDA+DMFT severely renormalizes the center of gravity of each band to $(\delta_x, \delta_y, \delta_z) = (-3.76, -2.93, -6.65)$ eV, as well as the orbital occupancies to $(n_\sigma^x, n_\sigma^y, n_\sigma^z) = (0.69, 0.78, 0.56)$, promoting enhanced orbital polarization. This fact, generic to multi-orbital systems (though we do not find total orbital polarization)⁴³, is an interesting manifestation of correlation-induced orbital rearrangement, and controls structural changes across the Mott transition (see below).

We now turn to the insulator-metal transition in solid O_2 at high P , and adopt the following strategy to derive this transition. Instead of reverting back to the LDA to use a different LDA density-of-states corresponding to the metallic ζ -phase, we search for an instability of the insulating, ε phase to the paramagnetic-metal by varying δ_a , found for the Mott insulator above. To proceed, consider the orbital-dependent on-site energy term, $H_\Delta = \sum_{i,a,\sigma} \Delta_a n_{i\sigma}^a$ in our Hamiltonian. We now let the trial Δ vary in small steps,

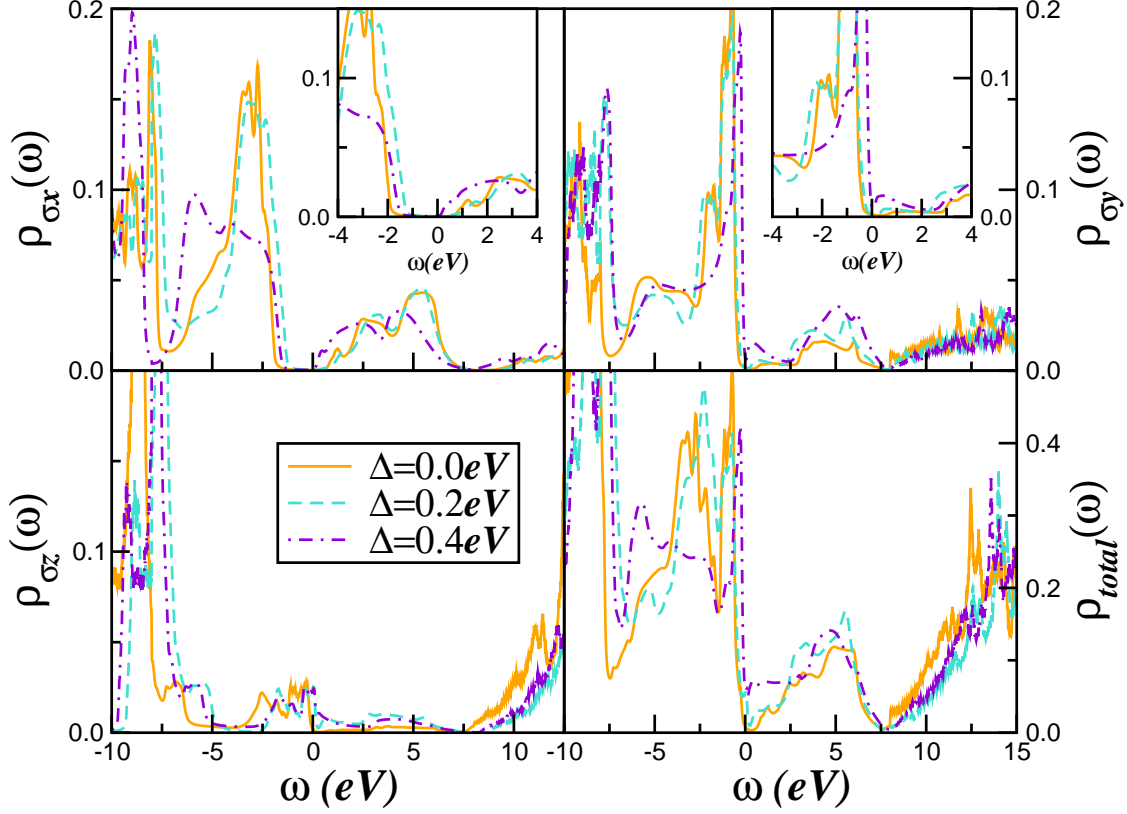


Figure 4 | Orbital-selective insulator-to-metal transition in pressurized O₂. In our theory, we vary the trial orbital-splitting Δ within LDA+DMFT to simulate structural changes upon pressure. In our results for the orbital-selective metallic phase the p_y (and hence, total) DOS shows a clear pseudogap around E_F , corresponding to an orbital-selective, non-Fermi liquid metallic phase. Inset at the top panels show the evolution of the electronic states close to the Fermi energy.

keeping $\Delta_x = -\Delta$, $\Delta_y = \Delta$, to simulate the structural (and hence, electronic) changes upon pressure. As for V₂O₃³⁸ and YTiO₃⁴², we search for the second self-consistent LDA+DMFT solution by solving the multi-orbital DMFT equations for each trial value of Δ keeping U, U' fixed. As seen in Fig. 4, small variations of Δ drive appreciable spectral weight transfer, producing drastic orbital-selective renormalizations of the one-particle spectral functions: the p_x and p_y are most severely affected. At a critical $\Delta_c = 0.3$ eV, the p_x density-of-states remains Mott insulating, while the p_y band undergoes an insulator to bad-metal (weakly first-order, with no coherent Kondo peak at E_F) transition. Thus, our results imply that the paramagnetic, metallic phase of ζ -oxygen is an orbital-selective incoherent metal without Landau quasiparticles, characterized by a pseudogap at E_F in the p_y , and hence, in the total spectral function, at E_F . Our simulations (not shown) indicate that Kondo-like resonance found below E_F for $\Delta = 0.4$ eV will cross the Fermi level at extremely high pressures, driving solid O₂ into (quasi)coherent Fermi liquid-like metallic state at even higher (experimentally uninvestigated) pressures. The underlying theoretical reason for this is as follows: At Δ_c , strong scattering between the effectively (Mott) localized and itinerant components of the matrix DMFT propagators produces an incoherent metal because strong interband scattering indeed operates in a sizably orbitally polarized metallic system. However, at very high pressure (large $\Delta > \Delta_c$), the p_x band becomes almost fully polarized (Fig. 5, upper panel) and the system evolves into a low- T correlated Fermi liquid metal⁴², which we predict to be the post- ζ phase. This is consistent with the fact that strong crystal-field splitting suppresses local orbital fluctuations and cuts off the strong scattering channel. In turn, this controls the orbital-selective phase boundary of correlated multi-orbital systems⁴⁴. From our results, the orbital-selective Mott phase is thereby suppressed at high pressure, leading to continuous evolution of the incoherent, bad-metal to a correlated Fermi liquid like metal.

In Fig. 5 we show the evolution of the orbital occupations n_σ^a (top) and the renormalized orbital splittings δ_a across the insulator-metal transition. The features are well understood as follows. In a multiband situation, Δ acts like an external ‘‘Zeeman’’ field^{38,42} in the orbital sector. The insulator-metal transition is characterized by a sudden jump in the renormalized δ_z , and in the p_x and p_y populations as a consequence, suggesting that anisotropic structural (and volume) changes will accompany the orbital-selective Mott transition. Here, we propose that these changes in n^a control anisotropic changes in lattice parameters ($\mathbf{a}, \mathbf{b}, \mathbf{c}$) across the insulator-metal transition: indeed, the changes in $\mathbf{a}, \mathbf{b}, \mathbf{c}$ are expressible in terms of n^a as $\gamma_a = \Delta l^a / l^a = (\frac{g}{M v_{sa}^2}) \Delta n^a$, where g is the electron-phonon coupling constant, M the ion mass, and v_{sa} is the velocity of sound along a ($\equiv x, y, z$). Changes in γ_a across the

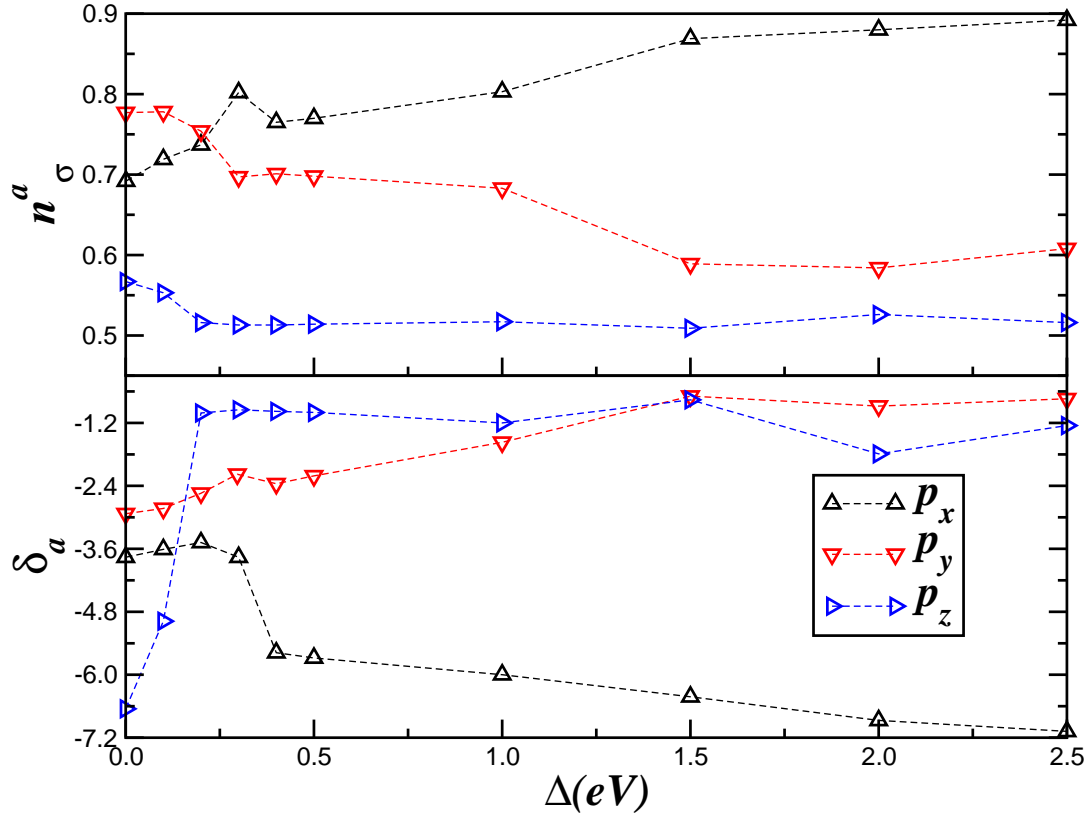


Figure 5 | Effect of the orbital “Zeeman” field upon pressure. (Top) LDA+DMFT results for the orbital occupations n^a and (bottom) the renormalized orbital splittings δ_a . Notice that n^y jumps at the insulator-metal transition, a behavior characteristic of orbital-selective Mott transition.

insulator-to-metal transition thus follow those in the n^a . Though values of v_{sa} and g in the ε phase are unknown, we deduce that the lattice parameter \mathbf{a} increases, while \mathbf{b}, \mathbf{c} decrease across the orbital-selective Mott transition as in Fig. 5 upper panel. The correct trend vis-a-vis experiment¹⁰ provides further support for our Mottness scenario in solid O₂.

Normal state resistivity

To illustrate the importance of correlation-induced changes in the orbital “Zeeman” field Δ under high pressure in our theory, we now discuss our results for the normal state resistivity computed within the Kubo formalism⁴⁵. In our theory, the observed features in $\rho_{dc}(T)$ originate from changes in the correlated spectral functions with Δ . Showing how this provides a compelling description of the admittedly limited available data is our focus in what follows. In Fig. 6, we show the $\rho_{dc}(T)$ for three values of Δ in solid O₂, computed using the LDA+DMFT orbital resolved spectral functions (with $U = 11.3$ eV, $U' = U - 2J_H$, and $J_H = 0.45$ eV). Various interesting features immediately stand out. First, $\rho_{dc}(T \rightarrow 0)$ in the ε phase ($\Delta = 0$) shows semiconducting behavior, in accord with the insulating classification at lower pressures, when $\Delta < \Delta_c$. Secondly, at all T , no Fermi liquid T^2 -like contribution is detectable in the metallic phase with $\Delta = 0.4$ eV: instead, $\rho_{dc}(T)$ is approximately constant up to 10 K. For intermediate pressure (but on the metallic side), $\rho_{dc}(T)$ crosses over from semiconductor-like (at high T) to bad-metallic (at low T) behavior. Remarkably, the detailed T -dependence closely resembles that seen in experiment⁹, in the normal state up to 2 K (see inset of Fig. 6). Since the system is proximate to a Mott transition, the T -dependence of $\rho_{dc}(T)$ for both values of $\Delta = 0.2, 0.4$ eV is characteristic for carriers scattering off dynamically fluctuating and coupled, short-range spin and charge correlations. On general grounds, we expect this effect to be relevant near a correlation-driven Mott transition. Since an external magnetic field will generically quench spin fluctuations, we predict that destroying the ε Mott insulating state by a magnetic field⁴⁶ might reveal this behavior. We emphasise that resistivity measurements as a function of pressure over extended T scales is a smoking gun for our proposal, as would be the study of the T -dependence of the dc Hall constant. These can distinguish a band-versus-Mott scenario for the pressure-induced insulator-metal transition: in the band-insulator-to-metal transition, there is no reason why, e.g. $\rho_{dc}(T)$ should show the above form, since neither orbital selectivity nor local antiferromagnetic spin fluctuations are operative there. More detailed transport work to corroborate our prediction are thus called for in future.

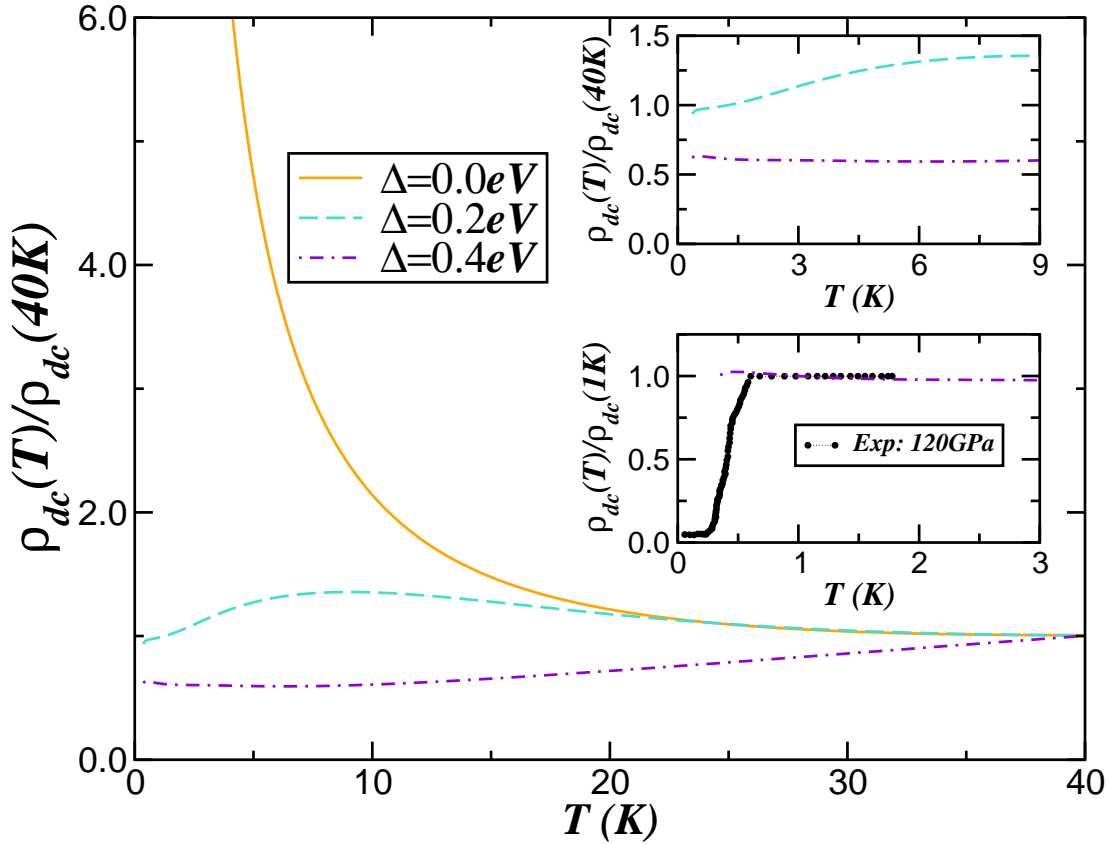


Figure 6 | Electrical resistivity of solid O_2 at high pressures. Main panel: Normal state resistivity versus temperature (normalized to $\rho(40\text{K})$), showing the metal-insulator transition with increasing the orbital “Zeeman” field Δ . Inset shows resistivity at very low temperatures: Observed features at low- T are well reproduced by strong Coulomb correlations U, U' and $\Delta = 0.4$ eV. Notice that results with small Δ value deviates from observation of constant $\rho(T)$ at 120 GPa in experiment⁹. It is possible that a detailed experimental study of $\rho_{dc}(T)$ in the pressure range closer to the insulator-to-metal transition may reveal the trend we find, and this would constitute more concrete support for our modelling.

III. DISCUSSION AND CONCLUSION

Insofar as superconductivity arises at the boundary of the Mott transition, our analysis provides tantalizing insight into sources of the pairing glue. Since the incoherent metal has a finite residual entropy ($S \propto \ln 2$ per site) from the Mott localized p_x sector, this electronic system is inherently unstable to soft two-particle instabilities⁴⁷. In solid O_2 at high pressure, lack of conditions supporting magnetic and charge-density instabilities in the correlated electronic structure near the insulator-metal transition opens the door to superconductivity as the only two-particle instability that can quench this finite normal state entropy. In fact, the situation is quite similar to that considered by Capone *et al.*⁴⁸ in the fulleride context, where the pseudogapped, bad metal arose from an unstable (intermediate coupling) fixed point in the impurity problem, corresponding to the Kondo unscreened phase: in our case, precisely the same effect results from selective localization of the p_x band at the orbital-selective Mott phase. In fact, in the orbital-selective metal, the low-energy physics is selfconsistently controlled by strong scattering between quasi-itinerant $p_{y,z}$ and Mott localized p_x orbital states, implying low-energy singularities in one- and two-particle propagators⁴⁹. This suggests soft, multi-orbital electronic modes at low energy, which can potentially act as a pair glue. In a way similar to the fulleride case, we then expect that multiband spin-singlet s -wave superconductivity (notice that $J_H \ll U$, favoring $S = 0$), driven by such soft inter-orbital electronic fluctuations in this unstable phase, will cut off the incoherent metal found above, and that the superconducting transition temperature T_c will rise to values larger than those obtained for the weakly correlated case⁴⁸. Interestingly, the variation of T_c with decreasing U/W (increasing pressure) found by Capone *et al.* does bear uncanny resemblance (Fig. 4 of ref. 48) to the $T_c(P)$ observed in solid O_2 under high pressure. This is suggestive, but out of scope of the present work. We leave details for the future.

In conclusion, we have theoretically studied the insulator-metal transition in highly pressurized solid O_2 using first-principles local-density-approximation plus dynamical-mean-field calculations. In analogy with multi-orbital d - and f -band systems, we find an orbital-selective Mott transition and an incoherent metallic normal state, arising from the Mott insulator via a weakly first-order transition as a function of pressure. Implications of our picture for the superconducting state are discussed: we propose that soft, multi-orbital electronic fluctuations involving dualistic states, i.e. the quasi-itinerant (p_y, p_z) and Mott localized (p_x) states arising at this orbital-selective Mott transition act as the pairing glue for the superconducting state found at low T in solid O_2 . Our work underlines the importance of local dynamical correlations in this molecular-solid system, and holds promise for understanding similar physics in other solidified gases.

Methods

To reveal the electronic reconstruction at the border of the Mott metal-insulator transition in solid Oxygen, we employ an state-of-the-art implementation of LDA+DMFT, which correctly takes disorder, temperature and pressure effects into account, in multi-band

systems³⁸. The one-particle, LDA density-of-states are computed using the non-fully relativistic version of the PY-LMTO code³³. To incorporate the effects of dynamical electronic correlations in solid O₂, we use the multi-orbital iterated-perturbation-theory (MO-IPT) as an impurity solver of the many-particle problem in DMFT³⁷. Finally, we carried out the computation of electrical transport within the Kubo formalism⁴⁵.

References

1. Mott, N.F. *Metal-insulator transitions*. (Taylor and Francis, London, 1974).
2. Ashcroft, N.W. Pairing instabilities in dense hydrogen. *Phys. Rev. B* **41**, 10963 (1990).
3. Edwards, B. & Ashcroft, N.W. Spontaneous polarization in dense hydrogen. *Nature* **388**, 652 (1997).
4. Lundegaard, L.F. *et al.*, Observation of an O₈ molecular lattice in the O₈ phase of solid oxygen. *Nature* **443**, 201 (2006).
5. Militzer, B. & Hemley, R.J. Crystallography: Solid oxygen takes shape. *Nature* **443**, 150 (2006).
6. Drozdov, A.P. *et al.*, Conventional superconductivity at 203 kelvin at high pressures in the sulfur hydride system. *Nature* **525**, 73 (2015).
7. Katzke, K. & Tolédano, P. Theory of the mechanisms of pressure-induced phase transitions in oxygen. *Phys. Rev. B* **79**, 140101(R) (2009).
8. Desgreniers, S., Vohra, Y. & Ruoff, A. Optical response of very high density solid oxygen to 132 GPa. *J. Phys. Chem.* **94**, 1117 (1990).
9. Shimizu, K. *et al.*, Superconductivity in oxygen. *Nature (London)* **393**, 767 (1998).
10. Weck, G. *et al.*, Single-crystal structural characterization of the metallic phase of oxygen. *Phys. Rev. Lett.* **102**, 255503 (2009).
11. Fujihisa, H. *et al.*, O₈ cluster structure of the epsilon phase of solid oxygen. *Phys. Rev. Lett.* **97**, 085503 (2006).
12. Eters, R.D., Helmy, A.A. & Kobashi, K. Prediction of structures and magnetic orientations in solid α - and β -O₂. *Phys. Rev. B* **28**, 2166 (1983).
13. Stephens, P.W. & Majkrzak, C.F. Magnetic structure and dynamics in the alpha and beta phases of solid oxygen. *Phys. Rev. B* **33**, 1 (1986).
14. Crespo, Y., Fabrizio, M., Scandolo, S. & Tosatti, E. Collective spin 1 singlet phase in high-pressure oxygen. *PNAS USA* **111**, 10427 (2014).
15. da Silva, A.J.R. & Falicov, L.M. Many-body calculation of the magnetic, optical, and charge-transfer spectra of solid oxygen in the α and β phases. *Phys. Rev. B* **52**, 2325 (1995).
16. Bao, W. *et al.* Magnetic correlations and quantum criticality in the insulating antiferromagnetic, insulating spin liquid, renormalized Fermi liquid, and metallic antiferromagnetic phases of the Mott system V₂O₃. *Phys. Rev. B* **58**, 12727 (1998).
17. Ma, Y. Artem R. Oganov, A.R. & Glass, C.W. Structure of the metallic ζ -phase of oxygen and isosymmetric nature of the ε - ζ phase transition: Ab initio simulations. *Phys. Rev. B* **76**, 064101 (2007).
18. Goncharenko, I.N. Evidence for a magnetic collapse in the epsilon phase of solid oxygen. *Phys. Rev. Lett.* **94**, 205701 (2005).
19. Serra, S. *et al.* Pressure-induced magnetic collapse and metallization of molecular oxygen: The ζ -O₂ phase. *Phys. Rev. Lett.* **80**, 5160 (1998).
20. Neaton, J.B. & Ashcroft, N.W. Low-energy linear structures in dense oxygen: Implications for the ε phase. *Phys. Rev. Lett.* **88**, 205503 (2002).
21. Ochoa-Calle, A.J., Zicovich-Wilson, C.M. & Ramírez-Solis, A. Solid oxygen γ phase and its transition from ε phase at extremely high pressure: A first-principles analysis. *Phys. Rev. B* **92**, 085148 (2015).
22. Tse, J.S. *et al.* Electronic structure of ε -oxygen at high pressure: GW calculations. *Phys. Rev. B* **78**, 132101 (2008).
23. Bartolomei, M. *et al.* Can density functional theory methods be used to simulate the ε phase of solid oxygen? *Chem. Phys. Letts.* **592**, 170 (2014).
24. Shih, B.-C. *et al.* Quasiparticle band gap of ZnO: High accuracy from the conventional G^0W^0 approach. *Phys. Rev. Lett.* **105**, 146401 (2010).
25. de' Medici, L. *et al.* Orbital-Selective Mott Transition out of Band Degeneracy Lifting. *Phys. Rev. Lett.* **102**, 126401 (2009).
26. Chan, J.A., Lany, S. & Zunger, A. Electronic correlation in anion p orbitals impedes ferromagnetism due to cation vacancies in Zn chalcogenides. *Phys. Rev. Lett.* **103**, 016404 (2009).
27. Winterlik, J. *et al.* Challenge of magnetism in strongly correlated open-shell $2p$ systems. *Phys. Rev. Lett.* **102**, 016401 (2009).
28. Wehling T.O. *et al.* Strength of effective Coulomb interactions in graphene and graphite. *Phys. Rev. Lett.* **106**, 236805 (2011).
29. Craco, L., Sellì, D., Seifert, G. & Leoni, S. Revealing the hidden correlated electronic structure of strained graphene. *Phys. Rev. B* **91**, 205120 (2015).
30. Chiappe, G., Louis, E., SanFabián, E. & Verges J.A. Hubbard Hamiltonian for the hydrogen molecule. *Phys. Rev. B* **75**, 195104 (2007).
31. Kotliar, G. *et al.* Electronic structure calculations with dynamical mean-field theory. *Rev. Mod. Phys.* **78**, 865 (2006).
32. Andersen, O.K. Linear methods in band theory. *Phys. Rev. B* **12**, 3060 (1975).
33. See, for example, Chadov S. *et al.* Tunable multifunctional topological insulators in ternary Heusler compounds. *Nature Mater.* **9**, 541 (2010).
34. Self-consistency was reached on a $14 \times 14 \times 12$ k -mesh for the Brillouin-zone integration. The radii of the atomic spheres were chosen as $r = 1.41$ for each O site, with empty spheres added. The LDA Perdew-Wang parametrization was used. Explicit inclusion of d -states in the valence do not change the LDA DOS.
35. Meng, Y. *et al.* Inelastic x-ray scattering of dense solid oxygen: Evidence for intermolecular bonding. *PNAS USA* **105**, 11640 (2008).
36. Kotliar, G. *et al.* Electronic structure calculations with dynamical mean-field theory. *Rev. Mod. Phys.* **78**, 865 (2006).
37. Craco, L. Quantum orbital entanglement: A view from the extended periodic Anderson model. *Phys. Rev. B* **77**, 125122 (2008).
38. Laad, M.S., Craco, L. & Müller-Hartmann, E. Orbital-selective insulator-metal transition in V₂O₃ under external pressure. *Phys. Rev. B* **73**, 045109 (2006).
39. Craco, L. & Leoni, S. Bulk quantum correlations and doping-induced nonmetallicity in the Bi₂Se₃ topological insulator. *Phys. Rev. B* **85**, 075114 (2012).
40. Craco, L. & Leoni, S. Tunable Kondo-Mott physics in bulk Bi₂Te₂Se topological insulator. *Phys. Rev. B* **85**, 195124 (2012).
41. Craco, L. & Leoni, S. Magnetoresistance in the Spin-Orbit Kondo State of Elemental Bismuth. *Scientific Reports* **5**, 13772 (2015).
42. Craco, L. *et al.* Theory of the orbital-selective Mott transition in ferromagnetic YTiO₃ under high pressure. *Phys. Rev. B* **77**, 075108 (2008).
43. Liebsch, A. & Ishida, H. Subband filling and Mott transition in Ca_{2-x}Sr_xRuO₄. *Phys. Rev. Lett.* **98**, 216403 (2007).
44. de' Medici, L. *et al.* Orbital-selective Mott transition out of band degeneracy lifting. *Phys. Rev. Lett.* **102**, 126401 (2009).
45. Grenzbach, C., Anders, F. B. & Czycholl, G. Transport properties of heavy-fermion systems. *Phys. Rev. B* **74**, 195119 (2006).
46. Nomura, T. *et al.* Novel phase of solid oxygen induced by ultrahigh magnetic fields. *Phys. Rev. Lett.* **112**, 247201 (2014).
47. Laad, M. S. & Craco, L. Theory of multiband superconductivity in Iron pnictides. *Phys. Rev. Lett.* **103**, 017002 (2009).
48. Capone, M. *et al.* Strongly correlated superconductivity and pseudogap phase near a multiband Mott insulator. *Phys. Rev. Lett.* **93**, 047001 (2004).
49. Anderson, P.W. The 'strange metal' is a projected Fermi liquid with edge singularities. *Nature Physics* **2**, 626 (2006).

Acknowledgements

The authors acknowledge interesting discussions with E. Tosatti at the early stages of this work. This work was supported by CNPq (Proc. No. 307487/2014-8) and DFG SPP 1415. S.L. acknowledges ZIH Dresden for the generous allocation of computational time. L.C. thanks the Institut für Theoretische Chemie, Technische Universität Dresden, for hospitality. S.L. wishes to thank the DFG for a personal Heisenberg Grant (Heisenberg Program).

Author contributions

S.L. performed *ab initio* (LDA) calculations. L.C. conceived the project and performed LDA+DMFT calculations. M.S.L. and L.C. analyzed the LDA+DMFT results and wrote the manuscript. All authors discussed the results and reviewed the manuscript.

Additional information

Competing financial interests: The authors declare no competing financial interests.

Correspondence and requests for materials should be addressed to L.C. (lcraco@fisica.ufmt.br)